Hindawi
Journal of Engineering
Volume 2023, Article ID 9335814, 16 pages
https://doi.org/10.1155/2023/9335814

Research Article

Prediction of Biogas Yield from Codigestion of Lignocellulosic Biomass Using Adaptive Neuro-Fuzzy Inference System (ANFIS) Model

Moses Oluwatobi Fajobi,[1,2] **Olumuyiwa Ajani Lasode**,[1] **Adekunle Akanni Adeleke**,[3] **Peter Pelumi Ikubanni**,[4] **Ayokunle Olubusayo Balogun**,[4] **and Prabhu Paramasivam**[5]

[1]*Department of Mechanical Engineering, Faculty of Engineering and Technology, University of Ilorin, Ilorin, Nigeria*
[2]*Ladoke Akintola University of Technology, Open and Distance Learning Centre, Ogbomoso, Nigeria*
[3]*Nile University of Nigeria, Abuja, Nigeria*
[4]*Department of Mechanical Engineering, Landmark University, Omu-Aran, Nigeria*
[5]*Department of Mechanical Engineering, College of Engineering and Technology, Mattu University, Mettu, Ethiopia*

Correspondence should be addressed to Prabhu Paramasivam; prabhu.paramasivam@meu.edu.et

Received 5 September 2022; Revised 26 December 2022; Accepted 4 January 2023; Published 6 February 2023

Academic Editor: Hans Kristianto

One of the major challenges confronting researchers is how to predict biogas yield because it is a herculean task since research in the field of modeling and optimization of biogas yield is still limited, especially with the adaptive neuro-fuzzy inference system (ANFIS). This study used ANFIS to model and predict biogas yield from anaerobic codigestion of cow dung, mango pulp, and *Chromolaena odorata*. Asides from the controls, 13 experiments using various agglomerates of the selected substrates were carried out. Cumulatively (for 40 days), the agglomerate that comprised 50% cow dung, 25% mango pulp, and 25% *Chromolaena odorata* produced the highest volume of biogas, 4750 m^3/kg, while the one with 50% cow dung, 12.5% mango pulp, and 37.5% *Chromolaena odorata* produced the lowest volume of biogas, 630 m^3/kg. The data articulated for modeling were those of the optimum biogas yield. Data implemented for modeling comprised two inputs (temperature in Kelvin and pressure in kN/m^2) and one output (biogas yield). The Gaussian membership function (Gauss-mf) was implemented for the fuzzification of input variables, while the hybrid algorithm was selected for the learning and mapping of the input-output dataset. The developed ANFIS architecture was simulated at varied membership functions, MFs, and epoch numbers to determine the minimum root mean square error, RMSE, and maximum R-squared R^2 values. The one that fulfilled the conditions was considered to be the optimized model. The minimum RMSE and maximum R^2 values recorded for the developed model are 14.37 and 0.99784, respectively. The implication is that the model was able to efficiently predict not less than 99.78% of the experimental data. These results prove that the ANFIS model is a reliable tool for modeling data and predicting biogas yield in the biomass anaerobic digestion process. Therefore, the use of the developed ANFIS model is recommended for biogas producers and other allies for predicting biogas yield adequately.

1. Introduction

In recent times, the energy crisis has ravaged the world at large with perceived consequences on mankind and the environment. The place of energy applications in the developmental course of any nation cannot be overemphasized because it is highly fundamental to nation-building and sustainability. The prominent energy sources are fossil fuels such as petroleum, diesel, kerosene, and liquefied natural gas, among others [1]. The application of fossil fuels is accompanied by various environmental pollution, such as the greenhouse gas effect, depletion of the ozone layer, ecological challenges, and climate disturbance, among others [2, 3]. It is in this connection that the need arises for other

origins of alternative energy, which is capable of engineering sustainable development [4]. Biomass is categorized as organic or inorganic based on its compositions, most of which have been constituting a nuisance in the environment due to inappropriate waste disposal methods. With the use of pertinent energy conversion and recovery approaches such as pyrolysis, torrefaction, and anaerobic digestion, full energy optimization is realistic, especially biogas. Thus, energy retrieval from biomass without affecting the environment is recommended [5–8]. Biogas is characterized by colourless as well as flammable with a significant percentage of methane content (Table 1), which makes it a good substitute for conventional energy [9]. Anaerobic digestion is an energy recovery approach specifically used to convert biomass to biogas in an air-tight environment through a four-stage process that includes hydrolysis, acidogenesis, acetogenesis, and methanogenesis [10–13].

One of the new major challenges confronting researchers is how to predict biogas yield because it is an extremely difficult task since research in the field of modeling and optimization of biogas yield is still limited [11, 14]. Among other numerous conventional machine learning software which had previously been applied to predict biogas yield are the artificial neural network (ANN), genetic algorithm (GA), adaptive neuro-fuzzy inference system (ANFIS), and logistic methods. Dibaba et al. [15] used the ANN to model some anaerobic parameters and biogas yield. It was reported that the output tracked the targets consistently. This was confirmed by the R^2 values recorded for the chemical oxygen demand (COD) removal (0.9063), the total suspended solids (TSS) (0.9152), volatile fatty acid (VFA) (0.9557), and biogas yield (0.9152). Wang et al. [16] used machine learning for the prediction of biogas generation from organic biomass when codigested anaerobically. The multilayer perceptron (MLP) model was compared with the Tree-based Pipeline Optimization Tool (TPOT) model. TPOT ($R^2 = 0.72$) outperformed the MLP ($R^2 = 0.56$). About 10% root mean square error (RMSE) was recorded for the TPOT; however, 14% RMSE was recorded for the MLP test dataset. Dinneya-Onuoha and Oyoh [8] reported that the modified Gompertz model had a superior performance in biogas yield prediction with a 0.9949 R^2 value. Conversely, the logistic growth model had a much lower R^2 value of 0.9920 when used for the prediction of biogas yield. Because the model considered the interactions of the core factors that aid biogas generation, it is proposed to be a highly useful tool for the optimization of the anaerobic digestion process. Further refinements, however, are still essentially required for monitoring input and output parameters frequently. Fajobi et al. [17] reported that among the prominent input parameters that influence biogas yield (output) are temperature and pressure because they are crucial to the effective anaerobic digestion process. Because as the temperature increases the methanogens react within the confinement of the digester and the rate of biogas production is increased thus inducing pressure [3]. In this connection, advanced models that consider the understanding of complex anaerobic digestion systems and kinetics are necessary. Fuzzy and neural models had been previously applied in the process of monitoring and predicting biogas yield in anaerobic digestion [18]. ANFIS is a system that is leveraged on the first-order Sugeno fuzzy model. It implements either a backpropagation algorithm solely or the use of a hybrid learning algorithm in a situation whereby the neural-network adaptive potentials, as well as fuzzy logic qualitative nature, are found matched together [19]. ANFIS has also found diverse applications, especially in anaerobic digestion and biogas production [18–22], geomatics engineering [23, 24], civil engineering [25], biomedical sciences [26], and power engineering [27]. Thus ANFIS has demonstrated superior performance in the prediction and approximation of the nonlinear relationship between multi-input and output.

Table 1: Constituents of biogas [9].

Biogas component	Chemical formula	Composition (%)
Methane	CH_4	54.9 to 75
Carbon dioxide	CO_2	34.9 to 45
Nitrogen	N_2	0 to 1
Hydrogen	H_2	0 to 1
Hydrogen sulphide	H_2S	1 to 2
Oxygen	O_2	Insignificant amounts
Carbon monoxide	CO	Insignificant amounts

[19].

Heydari et al. [19] developed ANN and ANFIS models for the prediction of the biogas produced from spearmint essential oil wastewater treatment in an upflow anaerobic sludge blanket digester. The statistics of the ANN model were R^2-square, 0.956, RMSE, 2651 mL/d, and a relative RMSE of 0.234%. At the same time, the statistics of the ANFIS model were R^2-square, 0.975, RMSE, 3516 mL/d, and relative RMSE of 0.316%. These showed that the two artificial intelligence-based models were excellent tools for estimating biogas yield. Ikpe et al. [18] reported that the use of the ANFIS network for estimating and predicting biogas yield in anaerobic digestion systems is still scanty and requires further practical applications. Unlike other conventional models, the construction of ANFIS models is easier and requires less stress because the rules are implemented based on the data trend. Also, new datasets and seasonal changes are adaptable for the training of ANFIS models [22, 28]. Therefore, it facilitates flexible usability for the user so that the model can be modified and updated as and when due [22]. Given the human need for optimum energy recovery, quantitative and qualitative fuel, economic value, and resource administering, further research in machine learning for predicting biogas yield becomes highly essential. The novelty of this study is based on the conception that several biogas yields have been previously predicted with the use of machine learning; however, biogas yield from the codigestion of cow dung, mango pulp, and *Chromolaena odorata* using the ANFIS model is yet to be carried out. The combination of several biomass to form an agglomerate for anaerobic digestion has been reported to be sound and proactive, not for complementary purposes alone but also for enhanced biogas yield. This is because of the various inherent properties of biomass that are desirable for anaerobic digestion. If one property is lacking in one biomass, it is provided by the other [29]. This formed the rationale behind the choice and blending of cow dung, mango pulp, and *Chromolaena odorata*. Aside from that,

Table 2: Experimental biomass formulates.

S/N	Digester (code name)	Cow dung (kg)	Mango pulp (kg)	*Chromolaena odorata* leaves (kg)	Biomass weight (kg)	Water quantity (kg)	Working volume (kg)
1	*A*	8	—	—	8	16	24
2	*B*	—	8	—	8	16	24
3	*C*	—	—	8	8	16	24
4	*D*	4	1	3	8	16	24
5	*E*	4	2	2	8	16	24
6	*F*	4	3	1	8	16	24
7	*G*	4	4	—	8	16	24
8	*H*	3	4	1	8	16	24
9	*I*	2	4	2	8	16	24
10	*J*	1	4	3	8	16	24
11	*K*	—	4	4	8	16	24
12	*L*	1	3	4	8	16	24
13	*M*	2	2	4	8	16	24
14	*N*	3	1	4	8	16	24
15	*O*	4	—	4	8	16	24

green leaves (such as *Chromolaena odorata*), when blended with other lignocellulosic biomass, enhanced biogas production [17]. Also, at the moment, no ANFIS graphical user interface (ANFIS-GUI) has been developed for the selected biomass. Therefore, the objective of this study was to develop and evaluate the ANFIS-based model and ANFIS-GUI for predicting the biogas yield of cow dung, mango pulp, and *Chromolaena odorata*.

2. Methodology

2.1. Materials. The raw materials which served as biomass codigested in this study were cow dung (50%), waste mango pulp (25%), and *Chromolaena odorata* (25%), all obtained from Ogbomoso, Nigeria (8° 8′ 31.78″ N, 4° 1′ 42.69″ E). The biomass had previously been characterized through proximate, ultimate, and compositional analyses. The results of the analyses were reported by Fajobi et al. [17]. Each biomass (formulates) (Table 2) was pounded in a mortar with the aid of a pestle until a soggy mass is reached. The slurry was prepared such that the ratio of the biomass to water was 1 : 2 by weight and was stirred continuously to ensure homogeneity and proper bacteria activities on the organic matter [30]. The slurry was later screened through a sieve of 1 mm pore to remove the fibres and other foreign materials. Then, each resulting slurry was ingested into the digesters and hermetically sealed for proper anaerobic digestion under mesophilic conditions (Table 2). So, other temperature ranges (thermophilic and psychrophilic) were not considered in this study. A total of 40 days' hydraulic retention time (HRT) was observed while daily temperature and pressure were recorded for determining the biogas yield using equations (1)–(3) according to Ogunkunle et al. [31]:

$$R = \frac{R_0}{M} x\,\%\,\text{Composition}, \tag{1}$$

$$R_{\text{Mixture}} = R_{\text{CO}_2} + R_{\text{CH}_4}, \tag{2}$$

$$V = \frac{R_{\text{Mixture}}\, x\, T_{\text{Digester}}}{P_e}, \tag{3}$$

where R = specific gas constant of a gas, measured in J/kgK; R_o = universal gas constant, measured in J/kgK; M = molecular mass of peculiar gas; R_{Mixture} = sum of specific gas constants of CH_4 and CO_2 content of the produced biogas; P_e = digester daily pressure, measured in kN/m^2; T_{Digester} = digester daily temperature, measured in Kelvin; and V = specific volume of the daily biogas produced, measured in m^3/kg.

2.2. Anaerobic Digestion of Biomass. A total volume of 0.074 m^3 digester was designed and fabricated with the use of locally sourced materials. The digester was designed to suit the condition of an anaerobic digestion process (complete absence of oxygen). After loading the digester with the prepared slurry, the daily temperature (in Kelvin) was taken using the digital temperature data logger (model: 877 with a type *K* thermocouple), and the pressure (measured in kN/m^2) using the digital pressure gauge (model no: model CPG500 with a measuring range from 0.1 to +150 kN/m^2) between the hours of 1300 and 1400 on each day of the HRT. Biogas analyzer (model no: 920 Series Continuous Biogas Analyzer) was used to analyze the constituents of the biogas samples. The gathered data were then presented in a Microsoft Excel spreadsheet, 2016 version, and consequently exported to MATLAB (Matrix Laboratory, Software R2018 version) interface where it was modeled using the ANFIS tool.

2.3. Theoretical Background of Adaptive Neuro-Fuzzy Inference System (ANFIS). The ANFIS network was constructed to achieve the desired nonlinear mapping of experimental data made up of several input-output pairs of the target system. A data learning algorithm was carried out for parameter adjustments and to improve the network performance. This study also used a unique dataset for the verification of the developed model's generalization strength. The ANFIS structure has five layers with two inputs, x and y, as shown in Figure 1. The ANFIS is a black-box model that only supports the mapping of multiple inputs and a single output. The square nodes in Figure 1 are also acknowledged as adaptive nodes, which implies that they can be learned as well as adjusted to suit the data trend. However,

the circle nodes, referred to as fixed nodes, imply that the parameters are fixed. Generally, two fuzzy if-then rules commonly adopted for the ANFIS are shown in equations (4)–(10) [32]:

$$\text{Rule 1: if } x \text{ is } A_1 \text{ and } y \text{ is } B_1, \text{then } f_1 = p_1 x + q_1 x + r_1, \tag{4}$$

$$\text{Rule 2: if } x \text{ is } A_2 \text{ and } y \text{ is } B_2, \text{then } f_2 = p_2 x + q_2 x + r_2, \tag{5}$$

where A and B stand as value ranges defined by the user. The interpretations of the layers presented in Figure 1 are explained from subsection 2.3.1– 2.3.5. The interpretations of the layers presented in Figure 1 go thus:

2.3.1. Layer 1. It is a square node provided with a node function:

$$O_i^L = \mu_{Ai}(x). \tag{6}$$

Assuming x and y are the values of two typical inputs supplied at the two input nodes. The node subsequently transformed the supplied values to the membership functions such as Tri-mf (triangular mf), Trap-mf (trapezoidal mf), Gbell-mf (generalized-bell-shaped mf), Gauss-mf (Gaussian mf), Gauss2-mf (Gaussian2 mf), Pi-mf (pi-shaped mf), Dsig-mf (D-sigmoidal mf), and Psig-mf (P-sigmoidal mf). O_i^L represents the membership function of Ai, while x is the input parameter supplied to the node. A_i is the linguistic label connected with the node function.

2.3.2. Layer 2. This is where the incoming signal is multiplied before the product is sent out. Here, individual node output serves as the firing strength of a rule where W_i represents the membership function of A_i.

$$W_i = \mu_{Ai}(x)x\,\mu_{Ai}(y), \quad i = 1, 2. \tag{7}$$

2.3.3. Layer 3. (1) Circle Node. This is the circle node where the ratio of the i-th rule's firing strength to the sum of all rules' firing strengths is being calculated:

$$w_i' = \frac{w_i}{w_1 + w_2}, \quad i = 1, 2. \tag{8}$$

2.3.4. Layer 4. This is a square node with a peculiar node function:

$$\begin{aligned} O_i^4 &= w_i' f_i, \\ &= w_i'(p_i \mathrm{x} + q_i \mathrm{x} + r_i), \end{aligned} \tag{9}$$

where p, q, and r are the parameter sets for consequent, linear, and parameters, respectively.

2.3.5. Layer 5

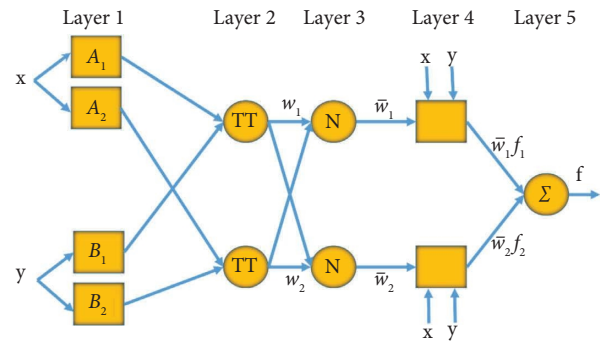

Figure 1: Equivalent ANFIS structure. (adapted from [22, 32, 33]).

(1) Circle Node. The addition of all incoming signals is being carried out here, and the resulting value represents the overall output.

$$\begin{aligned} O_i^5 &= \text{Overall output}, \\ &= \sum_i w_i' f, \\ &= \frac{\sum_i w_i f_i}{\sum_i w_i}. \end{aligned} \tag{10}$$

Concisely, layer 1 computes the membership grades, layer 2 combines the membership grades to form the firing strengths, layer 3 normalizes the firing strengths, layer 4 generates the contribution from each rule, and layer 5 produces the final output.

2.4. Modeling, Optimization, and Development of ANFIS for Predicting the Biogas Yield. Data implemented in the development of the ANFIS model were those recovered from codigestion of cow dung (50%), waste mango pulp (cherry species) (25%), and *Chromolaena odorata* (locally known as *Ewe Akintola*) (25%) of Ogbomoso origin (8°8′ 31.78″N, 4°1′42.69″E), in South-western Nigeria. The network architecture for this study was built to have a premise and consequent parameters. A hybrid learning algorithm was selected for the building and training of the ANFIS model using the MATLAB R2018 interface. The gathered experimental data were categorized into two parts. 70% of the experimental data was used to train the ANFIS model, while the remaining 30% was used for process testing and validation of the system [22]. To enhance the reliability of the model via data categorization, a MATLAB programming code was written to automatically, randomly categorize, and partition the data into training and testing as well as validation datasets such that the former was odd-indexed data points and the latter even-indexed data points, respectively. For this purpose, the collected daily digester's temperature (measured in kelvin) and pressure (measured in kN/m^2) values were induced as the input variables while biogas yield (measured in m^3/kg) was the predicted output. The membership function in the ANFIS is a function that brings back the membership degree of

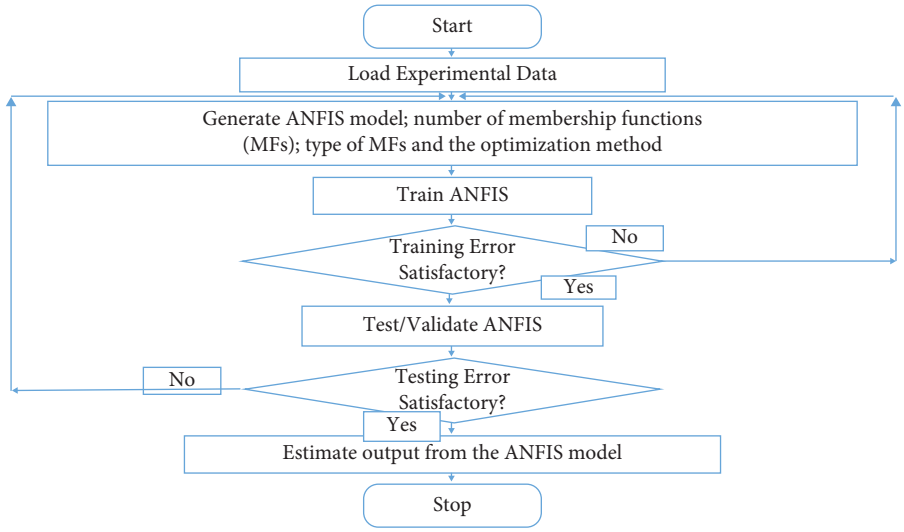

Figure 2: Computation flow chart implemented for ANFIS model development [38].

how a crisp (defined) value is mapped to an input space known as the universe of discourse. To determine the best fit ANFIS model, a total number of eight membership functions was used in the ANFIS structure training, with each input having seven numbers of membership functions, i.e., input 1 (temperature) and input 2 (pressure) having 7 and 7 numbers of membership functions, respectively. The following are the various membership functions (MFs) that were investigated before the optimized one was adopted considering the highest R^2, RMSE, and MAE values, namely; Tri-mf (triangular mf), Trap-mf (trapezoidal mf), Gbell-mf (Generalized-bell-shaped mf), Gauss-mf (Gaussian MF), Gauss2-mf (Gaussian2 mf), Pi-mf (pi-shaped mf), Dsig-mf (D-sigmoidal mf), and Psig-mf (P-sigmoidal mf). Grid partition was used to generate the ANFIS structure using 40 epochs. The training of the ANFIS structure was then actuated for model generation using the combinations of each membership function type and number, and the corresponding RMSE and MAE values were. A high number of membership functions performs adequately for the training of the model (overfitting). However, having a fewer number of membership functions may result in unsatisfactory convergence (underfitting) [34]. Therefore, to overcome these, this study used a trial and error method to determine the appropriate number of membership functions and epochs [35]. The epochs, membership functions, and numbers were adjusted systematically to overcome the overfitting and underfitting of the model. The selected membership functions are peculiar to ANFIS because they serve as the thinking faculty of the system, such that the reasoning of each of them differs [36]. Therefore, the motivation to investigate the choice membership functions was to determine the optimized ANFIS model when evaluated by the coefficient of determination, R^2 value, RMSE, and mean absolute error (MAE) because the lower the RSME and MAE, the higher and superior the model's predictions become [19]. Each type and number of the membership functions were simulated over the ANFIS architecture to arrive at the best ANFIS model. Each membership function is characterized by a shape that serves as each point in a specified input partition. For instance, Talpur et al. [37] stated that Gauss-mf with a curve utilizes only two parameters to optimize after the model's training such that c is used for locating the centre and σ was used to determine the width of the curve as expressed mathematically by equation (11). The highest R^2 value, least RMSE, and MAE indicated the optimized ANFIS model which was eventually used for the biogas yield predictions. Equation (12) was used to determine the training RMSE [22], and the R^2 value obtained for matching the experimental and predicted data was determined using equation (13) [33]. MAE was determined using equation (14) [34]. The computation flow chart used in this study for ANFIS model development is shown in Figure 2.

$$\text{gaussian}\,(x, c, \sigma) = e^{-(1/2)(x-c/\sigma)^2}, \tag{11}$$

$$\text{the RMSE} = \sqrt{\frac{1}{n}\sum_{i=1}^{n}(a_i - p_i)}^{2}, \tag{12}$$

where a_i represents the experimental value at instance i, p_i implies the predicted value at instance i, and n implies the number of training data points.

$$R^2 = \left[1 - \left(\frac{\sum_{i=1}^{n}(P^* - P)^2}{\sum_{i=1}^{n}(P_i^*)^2}\right)\right], \tag{13}$$

where P^* depicts the target value, and P depicts the model's predicted value.

$$\text{MAE} = \frac{1}{n}\sum_{i=1}^{n}|a_i - p_i|, \tag{14}$$

where a_i represents the experimental value at instance i, p_i implies the predicted value at instance i, while n implies the number of training data points.

2.5. Graphical User Interface for Predicting Biogas Yield. The graphical user interface development environment (GUIDE) tool embedded in MATLAB was used to develop the graphical user interface (GUI) for this study. This was used to lay out the interface of the developed biogas yield predictor GUI. The following features of GUIDE were used accordingly: static text box was selected for all the non-editable texts on the interface, such as the caption (biogas yield predictor), temperature (kelvin), and pressure (kN/m^2) and biogas yield (m^3/kg). An edit text box was used to present the unit for inputting the values of temperature and pressure (two yellow colour boxes). A static text box was selected for displaying the biogas yield (in the green box). Pushbutton was used to engineer the evaluation of the ANFIS model based on the input values. Therefore, once clicked, the corresponding biogas yield will be displayed in the yellow static text box. The GUI was adapted such that it is easy to navigate and determine the corresponding biogas yield on its interface. It was also developed such that it requires little or no technical know-how for its operation. Hence, domestic/commercial individuals who are or are not in the area of renewable energy studies, such as biogas production, can use it effectively for predicting the biogas yield.

3. Results and Discussion

3.1. Biomass and Biogas Characterizations. The results for the proximate, ultimate, and compositional analyses are presented in Table 3. The results are revelations of the suitability of the selected materials for anaerobic codigestion. Each exhibited the acceptable range of characteristics desired of typical biomass [17]. Therefore, they were considered appropriate, and consequently, their data were articulated for ANFIS modeling.

Figure 3 shows the biogas yields of the respective anaerobic codigestion of cow dung, mango pulp, and *Chromolaena odorata*. Cumulatively, formulate *E* (cow dung, 50%, mango pulp, 25%, and *Chromolaena odorata*, 25%) produced the highest volume of biogas, 4750 m^3/kg, while formulate *D* (cow dung, 50%, mango pulp, 12.5%, and *Chromolaena odorata*, 37.5%) produced the lowest volume of biogas, 630 m^3/kg. At the same time, other formulates produced biogas intermediately. Also, Table 4 compares the biogas yield of current and previous studies, and it showed that various biomass is/are viable feedstock for anaerobic sole or codigestion. Generally, the results showed that the combination of various lignocellulose biomass is a formidable and rich feedstock for anaerobic processes targeted at a high yield of biogas. Especially where the blends are adequate and proportionate. The results obtained from the analyses conducted on the various biogas samples of the experiments carried out and their calorific values are presented. It specifically presents the compositions of the biogas in terms of methane (CH_4), carbon dioxide (CO_2), hydrogen sulphide (H_2S), nitrogen (N_2), oxygen (O_2), and their water (H_2O) contents. A total number of 15 experiments (with code names; *A*, *B*, *C*, *D*, *E*, *F*, *G*, *H*, *I*, *J*, *K*, *L*, *M*, *N*, and *O*) was set up with cells *A*, *B*, and *C* being the control. Noteworthy is the fact that measurements for all the analyses were made thrice, with the averages taken as the true values. Table 5 shows the results of the analyses conducted on the biogas samples. It was observed that sample *O* had the lowest percentage oxygen content of 0.59%. This effect was obvious in the corresponding methane content obtained for the same sample, *O*, which stood at 66%. The percentage oxygen content present in all the biogas samples ranged between 0.59 and 0.91%, i.e., approximately all biogas samples had <1% of oxygen, respectively. These results align with those obtained in the literature for similar lignocellulose biomass used in this study [31, 51]. Furthermore, the percentage methane contents obtained for samples *I* and *K* were also relatively as high as those of *O*. These results may be due to the biomass formations that were fed into the digesters, which were a combination of three biomass for digester *I* (cow dung 25%, mango pulp 50%, and *Chromolaena odorata leave* 25%) and two biomass for*K* (50% each of mango pulp and *Chromolaena odorata*). The literature has it that combining two or more biomass as feedstock for anaerobic digestion promises to yield biogas within a short while and with richness in the methane content [52]. Therefore, the methane contents of 61.81 and 61.57% obtained from samples *I* and *K*, respectively, within the retention time could be attributed to balanced *C*/*N* among the biomass because they complement themselves in terms of carbon and nitrogen contents which is suitable for any adequate anaerobic digestion process. Asides from the process parameters which influenced biogas yield, the intermittent changes in feedstock characteristics achieved by agitations are worthy of note because it enhances the removal of scum on the surfaces of the slurries, aids the breakdown of organic matter, and improves nutrient balance in the mixtures. Also, the synergetic effects among the codigested biomass were suggested to be contributory factors. Despite all, the results obtained could still clearly indicate the significant effect of the mixing ratio on the methane yield. Generally, all the samples analyzed gave reliable results in terms of biogas constituents because none of them had methane content that was below 51%. This makes each biogas sample suitable for combustion resulting in very good calorific values. It is reported that for any biogas to combust effectively, it must have at least methane content ranging between 45 and 55% [12, 30]. Meanwhile, none of the ones obtained for this study was less than the limit set by the previous studies, with the methane content of many of the samples exceeding the higher set limit. However, it could be necessary to undertake a purification process to separate other constituents in the form of impurities from the biogas and to have biogas purer in the methane content.

3.2. Adaptive Neuro-Fuzzy Modeling of Biogas Production from Cow Dung, Mango Pulp, and Chromolaena Odorata. The scatter plot of the training and checking data after importing is presented in Figure 4. The two prominent parameters (temperature and pressure) reported by

Table 3: Biomass characterization.

Biomass	Cow dung	Mango pulp	*Chromolaena odorata*
Proximate analysis (%)			
Volatile matter (wet basis)	5.02	6.87	7.79
Volatile matter (dry basis)	60.75	62.78	71.49
Moisture content (wet basis)	85.82	85.77	83.11
Moisture content (dry basis)	10.98	11.35	9.89
Ash content (wet basis)	1.91	1.14	1.88
Ash content (dry basis)	5.60	3.85	5.12
Fixed carbon (wet basis)	7.25	6.22	7.22
Fixed carbon (dry basis)	22.67	22.02	13.50
VM/FC	0.69	1.10	1.07
Calorific values (MJ/kg)			
Calorific value	14.37	13.77	16.16
Ultimate analysis (%)			
Carbon (C)	43.08	39.98	41.69
Hydrogen (H)	7.87	6.74	9.86
Nitrogen (N)	1.53	1.34	1.51
Sulphur (S)	0.46	0.12	0.25
Oxygen (O)	47.06	51.82	46.69
C/*N* ratio (no unit)	28.16	29.84	27.61
H/*C* (no unit)	0.19	0.17	0.24
O/*C* (no unit)	1.09	1.29	1.12
Compositional analysis (%)			
Hemicellulose	10.76	7.47	11.37
Lignin	6.33	0.22	0.90
Cellulose	12.03	3.71	5.15
%NDF	41.69	47.90	49.80
%ADF	29.19	40.70	32.78

*Values represent the average value for respective analyses (Source: [17]).

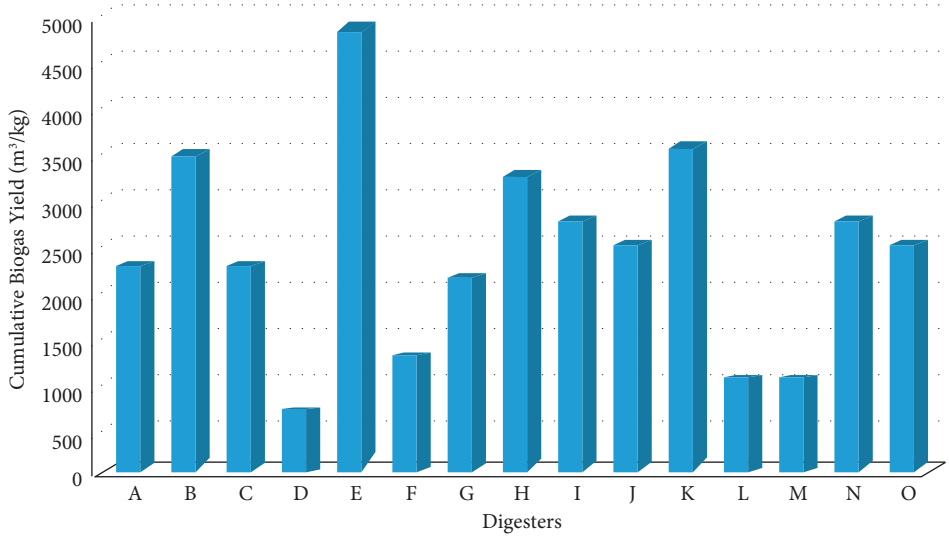

Figure 3: Cumulative (40 days) biogas production for each of the digesters [38].

previous studies were also confirmed in this study to strongly influence biogas production [45, 51]. Figure 4 presents the positions of each data point relative to the other in the ANFIS network. It revealed that the training data matched those of the checking data within the context.

3.3. Optimization of Membership Functions and Generation of ANFIS Structure. Table 6 shows that Tri-mf, Trap-mf, Gbell-mf, Gauss-mf, Gauss2-mf, Pi-mf, Dsig-mf, and Psig-mf has RMSE values of 117.55, 173.77, 186.09, 14.37, 169.22, 52.63, 41.72, and 47.12, respectively. And MAE values 6.8213, 9.0987, 12.2345, 2.3123, 7.9057, 5.8726,

Table 4: Comparison of methane yield of previous and present study.

Biomass	Pretreatment	Methane yield	Reference
Cow dung	Untreated	6.50 L	Zulkifi et al. [39]
Cow dung	Screening (enzymatic hydrolysis process)	6.91 L	Zulkifi et al. [39]
Plantain peels	NR	<30 mL	Makinde and Odokuma [40]
Plantain peels and cow dung	NR	>30 mL	Makinde and Odokuma [40]
Yam peels	NR	<35 mL	Makinde and Odokuma [40]
Yam peels and cow dung	NR	>35 mL	Makinde and Odokuma [40]
Shorea wood waste and cow dung	Soaking and filtration	1999 mL against 822 mL (individual digestion)	Amirta et al. [41]
Grass and cow dung	Untreated	179.59 mL CH_4/g VS_{added}	Prapinagsorn et al. [42]
Silage and cow dung	Untreated	208.11 mL CH_4/g VS_{added}	Prapinagsorn et al. [42]
Grass and cow dung	Alkaline plus enzyme treatment	333.63 mL CH_4/g VS_{added}	Prapinagsorn et al. [42]
Silage and cow dung	Alkaline plus enzyme treatment	301.38 mL CH_4/g VS_{added}	Prapinagsorn et al. [42]
Cow dung	NR	1301.7 IN CH_4 kg^{-1} FM	Ogunkunle et al. [31]
Cow dung and jatropha cake	NR	2656.0 IN CH_4 kg^{-1} FM	Ogunkunle et al. [31]
Cow dung	NR	0.31 mL·kg	Asante-Sackey et al. [43]
Cow dung and miscanthus fuscus	NR	0.46 mL·kg	Asante-Sackey et al. [43]
Sawdust waste, cow dung, and water hyacinth	NR	8–9% CH_4 increment	Madu and Onwuamaeze [44]
Cow dung	Untreated	0.63–5.84 L/week	Kargwal et al. [45]
Cow dung and pawpaw straw	Pawpaw soaked	0.73–5.87 L/week	Kargwal et al. [45]
Cow manure	NR	439 mL/g VS_{added}	Wei et al. [46]
Maize straw	NR	198.33 mL/g VS_{added}	Wei et al. [46]
Cow manure and maize straw	NR	613.8 mL/g VS_{added}	Wei et al. [46]
Cow manure, maize straw, and sewage sludge	NR	8052.0 mL/g VS_{added}	Wei et al. [46]
Organics	Untreated	53%	Vrabie [47]
Petrochemicals	Untreated	56%	Vrabie [47]
Paper	Untreated	51%	Vrabie [47]
Wood	Untreated	52%	Vrabie [47]
Leather	Untreated	34%	Vrabie [47]
Cotton and wool	Untreated	65%	Vrabie [47]
Acacia leaf waste	Untreated	49.0 ± 5.3%	Hirunsupachote et al. [48]
Acacia leaf waste	Alkaline pretreatment	199.6 ± 9.0%	Hirunsupachote et al. [48]
Sewage sludge and organic fraction of municipal solid waste	Untreated	61%	Ferrentino et al. [49]
Water hyacinth (*Eichhornia crassipes*)	Untreated	213.92 mL g^{-1} VS	Keche et al. [50]
Cow dung	Untreated	62.52%	Present study [38]
Mango pulp	Untreated	51.81%	Present study [38]
Chromolaena odorata	Untreated	52.79%	Present study [38]
Cow dung and mango pulp	Untreated	52.89%	Present study [38]
Cow dung and *Chromolaena odorata*	Untreated	66.85%	Present study [38]
Mango pulp and *Chromolaena odorata*	Untreated	61.57%	Present study [38]

NR: not reported (a compilation of the [38]).

4.2914, and 4.7612, respectively. These depict that Gauss-mf has the least RSME (14.72) and MAE (4.2914) values. Consequently, the ANFIS structure for modeling and predictions was built using the Gauss-mf membership function because the ANFIS model, when developed with the minimal RMSE and MAE, i.e., ANFIS-Gauss-mf, gives actual prediction [53]. The plot of training and checking errors against the epoch number is shown in Figure 5. Training plot is in blue ink, while the checking plot is in brown ink. The optimized training RMSE is located in the small rectangle showing the coordinate (epoch number, 40, RMSE, 14.37) of the exact point

Table 5: Constituents' analyses of biogas samples [38].

Digesters (samples)	CH_4 (%)	CO_2 (%)	H_2S (%)	N_2 (%)	O_2 (%)	H_2O (%)
A	62.52	27.93	1.12	0.40	0.68	1.34
B	51.81	25.73	1.31	0.68	0.76	1.52
C	52.79	26.68	1.10	0.49	0.78	1.51
D	51.96	25.98	1.29	0.47	0.80	1.53
E	51.89	25.95	1.25	0.62	0.84	1.49
F	54.19	26.91	1.15	0.57	0.73	1.36
G	52.89	26.51	1.34	0.65	0.85	1.59
H	52.60	26.37	1.27	0.49	0.79	1.61
I	61.81	29.17	1.11	0.39	0.65	1.32
J	52.07	26.19	1.18	0.59	0.88	1.57
K	61.57	28.94	1.13	0.41	0.67	1.29
L	52.82	26.48	1.21	0.53	0.71	1.43
M	51.67	25.52	1.36	0.72	0.91	1.63
N	52.71	26.41	1.24	0.55	0.81	1.45
O	66.85	28.96	1.09	0.35	0.59	1.27

[18].

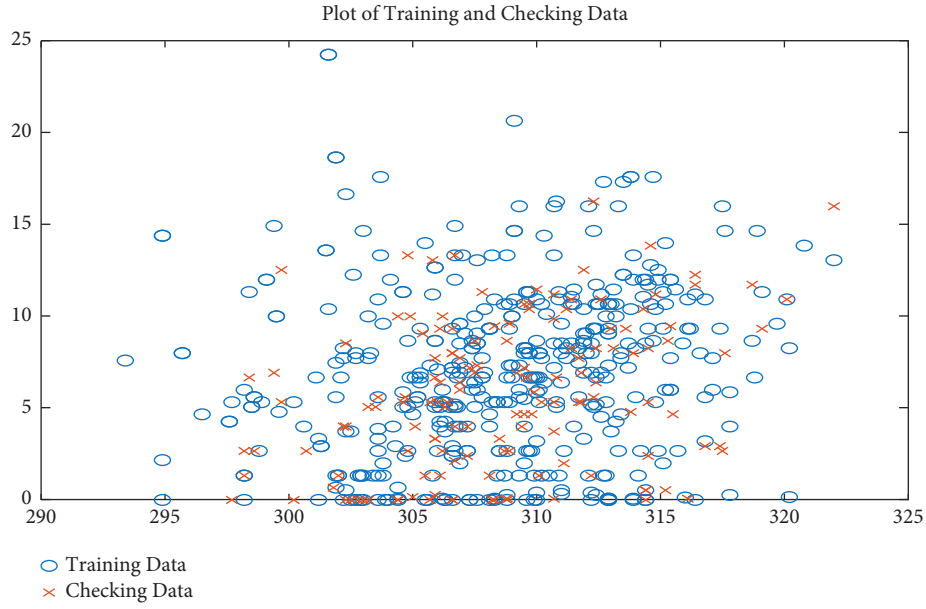

Figure 4: Scatter diagram of both the training and checking data.

Table 6: Optimization of ANFIS models.

Data point	Types of ANFIS models	No. of mf	Epoch	Training R^2 value	Training RMSE	Training MAE
160	ANFIS-Tri-mf	7, 7	40	0.6451	117.55	6.8213
160	ANFIS-Trap-mf	7, 7	40	0.3719	173.77	9.0987
160	ANFIS-Gbell-mf	7, 7	40	0.2837	186.09	12.2345
160	ANFIS-Gauss-mf	7, 7	40	0.9978	14.37	2.3123
160	ANFIS-Gauss2-mf	7, 7	40	0.4819	169.22	7.9057
160	ANFIS-Pi-mf	7, 7	40	0.7452	52.63	5.8726
160	ANFIS-Dsig-mf	7, 7	40	0.8451	41.72	4.2914
160	ANFIS-Psig-mf	7, 7	40	0.8107	47.12	4.7612

where ANFIS training stopped. Points after this imply that the data pattern is no more training the structure but it is memorizing the data.

Plots of inputs' initial and optimized Gauss-mf membership function for temperature (Supplementary A) and pressure (Supplementary B) are attached as supplementary materials. Before and after optimization, smooth curves are observable in the Gaussian membership function (Gauss-mf). Compared with before optimization, slight shifts in the curves were observed in each case. These are indications of

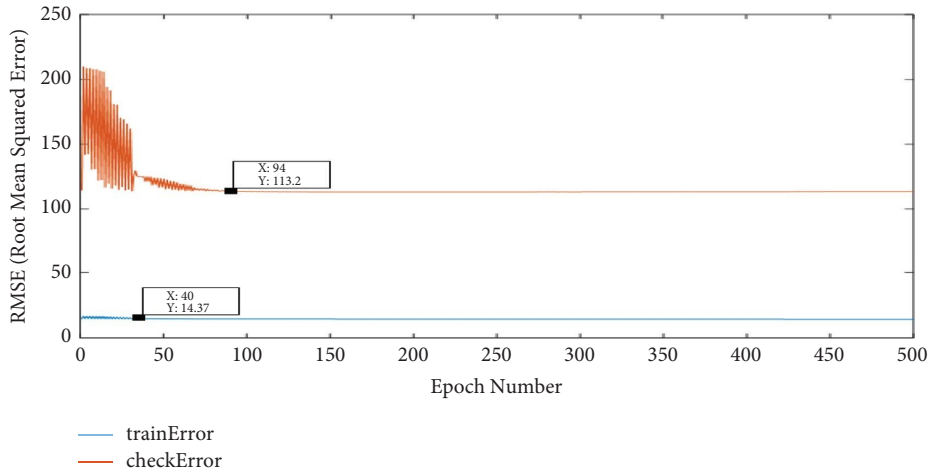

Figure 5: Error curves for training (blue) and checking errors (brown).

changes in the positions of the membership functions in terms of the degree of freedom relative to the dataset of pressure and temperature. This suggested the absolute judgement about the individual value of the dataset. Therefore, the ANFIS model predominantly utilized the pressure and temperature degradation signals for estimating the biogas yield. The ANFIS-Gauss-mf model structure that was developed with the use of the earlier optimized Gaussian membership function is represented in Figure 6. It was then used to model and predict the biogas yield. Evidently, from Figure 6, the input variables (temperature and pressure), membership function, rules, output membership function, and output (biogas yield) are in synergy with neurons. The observed neuron relationship is regarded as substantial, highly robust, and guarded against discrepancies. The structure has an excellent ability to learn the kinematics of the data used for the model development [53]. Artificial intelligence (AI) models, on the other hand, are a set of flexible structural interconnectivity in-between layers and nodes which are linked together to execute the desired function [54].

3.4. The Effectiveness of the ANFIS Model. The effectiveness of the developed ANFIS model for adequate predictions is demonstrated in Figures 7 and 8. Figure 7 shows a parity plot (regression analysis) where the ANFIS predicted data (vertical axis) and experimental data (horizontal axis) are designated on the x-axis and y-axis, respectively. Also, Figure 7 reveals that ANFIS prediction has an R^2 value of 0.99784. R^2 is a statistical index that is used in the regression model for the determination of the proportion of variance in factors (temperature and pressure) that can be accounted for by the output variable (biogas yield). It could also be inferred that the R^2 value depicts the level (the goodness of fit) to which the data fit the regression model. Fajobi et al. [55] reported that in statistics, the smaller RMSE metrics are an indication of the model's correctness, implying that it is better. However, a high R^2 value revealed the level of conformity degree amongst the experimental and the predicted data. It implies that 99.8% of the dependent (biogas yield) variable was accurately predicted by the independent variables, i.e., temperature and pressure. Figure 7 further substantiates this fact through the plot of qualitative prediction efficiency (plot of training data versus that of ANFIS output) of the ANFIS model. Two scenarios were presented therein: the first is the representation of typical accurate prediction, and the second are those that are almost accurately predicted. Affirmatively, all these proved the efficacy of the developed ANFIS model [36]. Two important measures often applied to establish the difference between the model predicted and the real data are the RMSE and MAE. They are also used to give a general overview of deviations as well as error distributions [52, 56]. The values of RMSE and MAE observable in Table 6 for the Gauss-mf are considered relatively small enough compared to others. They are sufficient to demonstrate that the error distributions for the ANFIS model are negligible. When the ANFIS model showed small error distributions, it is an indication of how reliable the projected data are. Furthermore, the developed ANFIS model was compared with other conventional models found in the previous studies to validate the developed model (Table 7). Observably, the developed ANFIS model was to a great extent effective, and it predicted biogas yield more efficiently compared to other models because it is just a few of the list in Table 7 has an R^2 value greater than that of the ANFIS model ($R^2 = 0.9978$). Also, the variability observed in the R^2 values could be attributed to the type of model, the methodology embraced, and the nature of the historical data that was modeled.

Mapping of input(s) to output, termed the fuzzy logic aspect of ANFIS modeling, requires essential rules, and the expected number of rules is expressed as K^d. The number of input membership functions is denoted by K, while the number of independent data input factors is denoted by d [36]. In this study, seven (7) numbers of membership functions were appropriated for each of the two inputs (meaning 7^2 for this study). Therefore, utilizing a 7 by 7 matrix resulted in a total of 49 rules generated by the ANFIS model. The set of rules is being triggered to make predictions upon the creation of the ANFIS structure. By this, other data

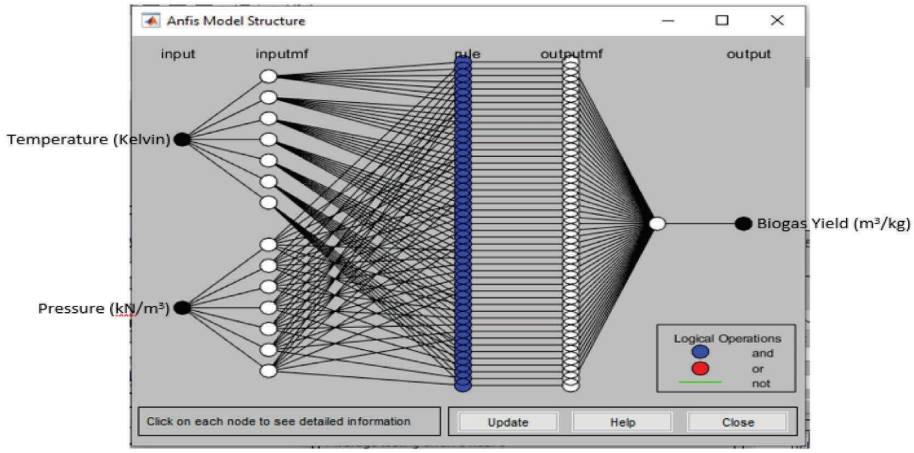

Figure 6: Generated ANFIS model structure for prediction.

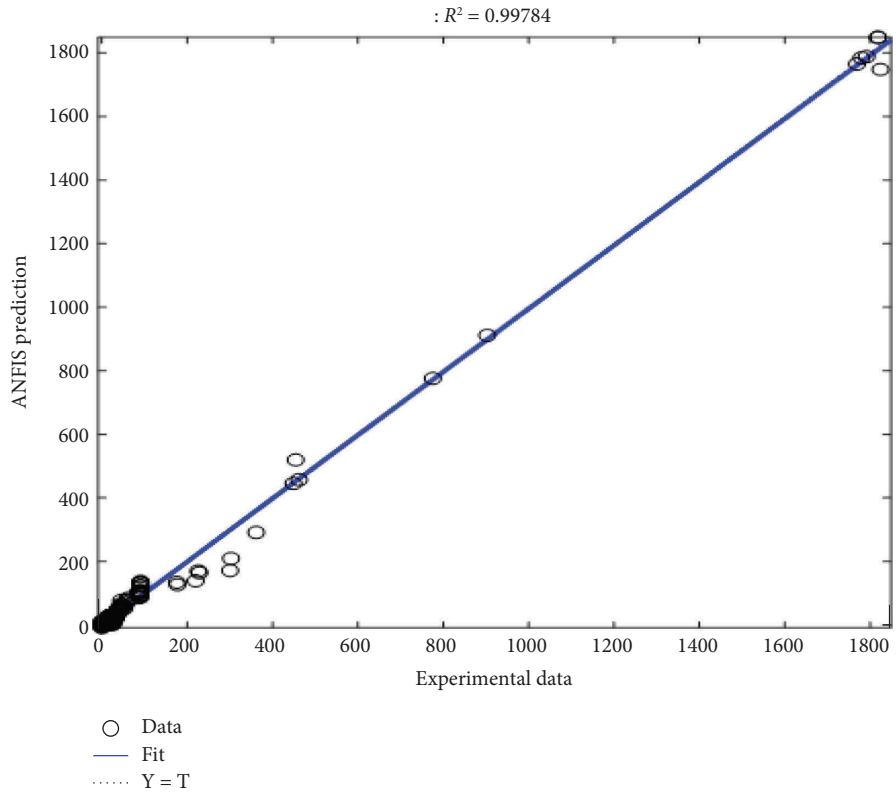

Figure 7: Effectiveness of the ANFIS prediction (parity plot).

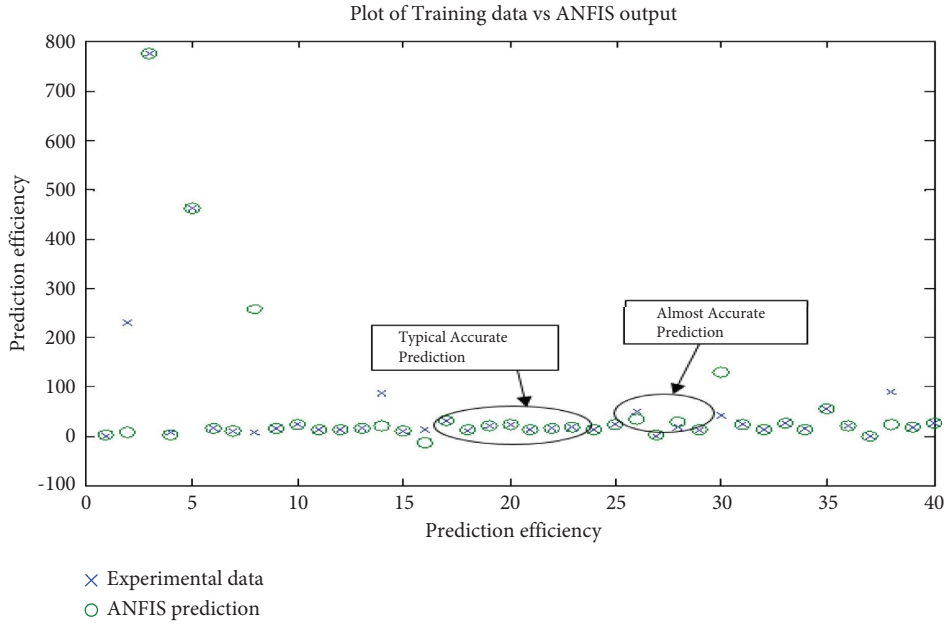

Figure 8: Effectiveness of the ANFIS prediction (qualitative plot).

Table 7: Comparison of developed ANFIS and previous models found in the literature.

Model type	Input	Output	Validation (R^2 value)	Reference
ANFIS	Delivery speed, break draft, and distance between the back and middle rolls	Breaking strength	0.4800	Fallahpour and Moghassem [57]
Gene expression programming (GEP) models	Delivery speed, break draft, and distance between the back and middle rolls	Breaking strength	0.8700	Fallahpour and Moghassem [57]
Multilayered feed-forward neural network	Mass amount of pineapple peel, pH of the inlet, COD of the inlet, volatile fatty acids (VFA) of the inlet, and volatile solids (VS) of the inlet	VS of the outlet, the volume of biogas, and the methane fraction of biogas	0.9942	Jaroenpoj et al. [58]
ANFIS	pH, temperature, time, yeast extraction concentration, and K_2HPO_4	Polygalacturonase activity	0.9780	Uzuner and Cekmecelioglu [59]
ANN	pH, temperature, time, yeast extraction concentration, and K_2HPO_4	Polygalacturonase activity	1.0000	Uzuner and Cekmecelioglu [59]
ANFIS	Cherry tomatoes, storage temperature, and storage time	Physicochemical and microbiological parameters	>0.86	Tao et al. [60]
ANFIS	Solar radiation, relative humidity, total dissolved solids of the feed, total dissolved solids of the brine, and feed flow rate	Solar still productivity	0.9900	Mashaly and Alazba [61]
ANFIS	Velocity distribution and CFD iteration time	Temperature	0.9990	Babanezhad et al. [62]
ANN	Cutting speed, feed rate, and depth of cut	Metal removal rate and tool wear	0.9210	Sada and Ikpeseni [63]
ANFIS	Cutting speed, feed rate, and depth of cut	Metal removal rate; tool wear	0.7300	Sada and Ikpeseni [63]
Bayesian-ANFIS	Class record and exam performance	Student performance	0.7990	Makolo and Olapojoye [64]
ANFIS	Temperature and pressure	Biogas yield	0.9978	Present study [38]

points that are beyond the scope of those experimentally obtained can be predicted accordingly. The trend observed is in proximity to that of the experimental data. The graphical user interface adapted to ease the projection of biogas yield upon supply of temperature in kelvin and pressure in kN/m^2 is presented in Figure 9.

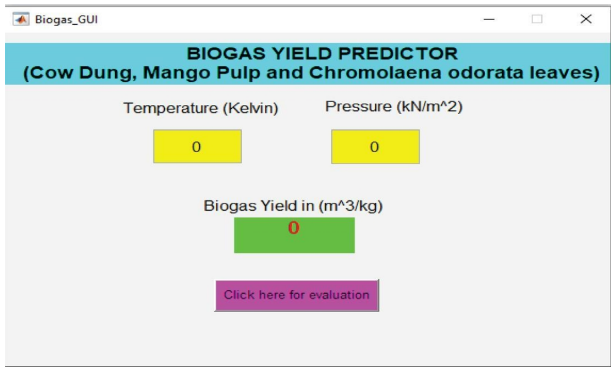

FIGURE 9: Graphical user interface, GUI for biogas yield prediction.

4. Conclusions and Recommendations

This study has developed an ANFIS model for efficient and accurate prediction of biogas yield from cow dung co-digested with mango pulp and *Chromolaena odorata*. Data collated from the anaerobic digestion of the selected biomass were modeled on the ANFIS. The results showed that the R^2, RMSE, and MAE values of the optimized ANFIS model are 0.99784, 14.37, and 2.3123, respectively. Furthermore, considering the effectiveness metrics of all the membership functions investigated, the Gaussian membership function is observed to have a good matching ability compared to the other membership functions. Compared to other conventional models, the ANFIS model had superior accuracy. However, the nature of the data and model development approach are considered factors that influenced the results. The GUI developed will aid the use of the ANFIS model by biogas producers. Therefore, this study recommends the use of the developed ANFIS model for the prediction of biogas yield. Biogas producers and allied will find, in this model, an adequate working tool for the optimization of biogas yield.

Nomenclature

ANFIS:	Adaptive neuro-fuzzy inference system
ANN:	Artificial neural network
CH_4:	Methane
CO:	Carbon monoxide
CO_2:	Carbon dioxide
COD:	Chemical oxygen demand
Dsig-mf:	D-sigmoidal membership function
E:	Error function
FIS:	Fuzzy inference system
FL:	Fuzzy-logic
Gauss2-mf:	Gaussian2 membership function
Gauss-mf:	Gaussian membership function
Gbell-mf:	Generalized-bell-shaped membership function
GUI:	Graphical user interface
GUIDE:	Graphical user interface development environment
H_2:	Hydrogen
H_2S:	Hydrogen sulphide
HRT:	Hydraulic retention time
J/kgK:	Joules per kilogram kelvin
K:	Kelvin
kN/m^2:	Kilonewtons per meter square
m^3/kg:	Meter cube per kilogram
M:	The molecular mass of the gas concerned
MFs:	Membership functions
MLP Network:	Multilayer perceptron network
MVR:	Multivariable regression
N_2:	Nitrogen
O_2:	Oxygen
OLR:	Organic loading rate
P:	Model's predicted value
P_e:	The estimated daily pressure of the digester
pH:	The acidity or alkalinity of the biomass
Pi-mf:	Pi-shaped membership function
Psig-mf:	P-sigmoidal membership function
R^2 value:	Coefficient of determination
MAE:	Mean absolute error
RMSE:	Root mean square error
R:	The specific gas constant of a gas
R_o:	Universal gas constant (J/kgK)
$R_{Mixture}$:	The total specific gas constant of the assumed biogas composition
R-value:	Coefficient of correlation
spec. GPR:	Specific gas production rate
TPOT:	Tree-based pipeline optimization tool model
Trap-mf:	Trapezoidal membership function
Tri-mf:	Triangular membership function
TSS:	Total suspended solids
V:	The specific volume of daily biogas generated in m^3/kg
VFA:	Volatile fatty acid
VS:	Volatile solid
VSS:	Volatile suspended solids inserted.

Data Availability

The data used to support the findings of this study are included within the article. Should further data or information be required, these are available from the corresponding author upon request.

Conflicts of Interest

The authors declare that they have no conflicts of interest.

Authors' Contributions

F.M.O. conceptualized the study, reviewed and edited the manuscript, proposed the methodology, performed investigation and data collection, formal data analysis, and production of the original draft. L.O.A. performed the provision of research materials, supervision, and reviewed the manuscript methodology. A.A.A. and P.P. performed manuscript review, editorials, and results and discussion. I.P.P. and B.A.O. carried out review and suggestions on the discussion of results. The manuscript was reviewed by all the

authors and unanimously approved the final copy for publication.

Acknowledgments

The authors would like to express gratitude to the Department of Mechanical Engineering, University of Ilorin, Ilorin, Nigeria, for creating the avenue to carry out the experimentation at the departmental premises. The authors appreciate the supports from Mattu University, Ethiopia. Also, their appreciations go to the enumerators who were trained and assisted in the data collection.

Supplementary Materials

Plots of input initial and optimized Gauss-mf membership function for temperature (A) and pressure (B) are attached as supplementary materials. Before optimization and after optimization of the model using the Gaussian membership function (Gauss-mf), smooth curves were observed. Compared with the optimization performed before, slight shifts in the curves were observed in each case. There is an indication of changes in the positions of membership functions in terms of the degree of freedom relative to the dataset of pressure and temperature. (*Supplementary Materials*)

References

[1] S. Zerrouki, R. Rihani, K. Lekikot, and I. Ramdhane, "Enhanced biogas production from anaerobic digestion of wastewater from the fruit juice industry by sonolysis: experiments and modelling," *Water Science and Technology*, vol. 84, no. 3, pp. 644–655, 2021.

[2] F. A. Aisien and E. T. Aisien, "Biogas from cassava peels waste," *Detritus*, vol. 10, pp. 100–108, 2020.

[3] S. O. Cinar, S. O. Cinar, N. Wieczorek, I. Sohoo, and K. Kuchta, "Integration of artificial intelligence into biogas plant operation," *Processes*, vol. 9, no. 1, p. 85, 2021.

[4] M. O. Fajobi, O. A. Lasode, A. A. Adeleke, P. P. Ikubanni, and A. O. Balogun, "Effect of biomass Co-digestion and application of artificial intelligence in biogas production: a review," *Energy Sources, Part A: Recovery, Utilization, and Environmental Effects*, vol. 44, no. 2, pp. 5314–5339, 2022.

[5] I. K. Adegun and S. S. Yaru, "Cattle dung biogas as a renewable energy source for rural laboratories," *Journal of Sustainable Technology*, vol. 4, no. 1, pp. 1–8, 2013.

[6] R. Alvarez and G. Liden, "Low-temperature anaerobic digestion of mixtures of llama, cow and sheep manure for improved methane production," *Biomass and Bioenergy*, vol. 33, no. 3, pp. 527–533, 2009.

[7] M. Belaid, A. N. Matheri, I. C. Lelosa, E. Muzenda, and I. Ramatsa, "Optimization of biogas production from sewage sludge," in *Proceedings of the International Conference on Industrial Engineering and Operations Management*, Bangkok, Thailand, March 2019.

[8] E. Dinneya-Onuoha and K. B. Oyoh, "Production, kinetics and purification of biogas from cow-dung and cassava peels," *International Journal of Electrical and Power Engineering*, vol. 15, no. 1, pp. 1–10, 2021.

[9] N. Norouzi and H. Khajehpour, "Simulation of methane gas production process from animal waste in a discontinuous bioreactor," *Biointerface research in applied chemistry*, vol. 11, no. 6, Article ID 13859, 2021.

[10] N. Ahmad Kamal, S. N. Osman, D. Y. Lee, and M. Ab-Wahid, "Analysis of biogas production from biomass residue of palm oil mills using an anaerobic batch test," *Sains Malaysiana*, vol. 50, no. 12, pp. 3583–3592, 2021.

[11] E. K. Peng, M. Abdul Malek, and S. M. Shamsuddin, "Artificial intelligence projection model for methane emission from livestock in Sarawak," *Sains Malaysiana*, vol. 48, no. 7, pp. 1325–1332, 2019.

[12] M. A. Olojede, O. Ogunkunle, and N. A. Ahmed, "Quality of optimized biogas yields from co-digestion of cattle dung with fresh mass of sunflower leaves, pawpaw and potato peels," *Cogent Engineering*, vol. 5, Article ID 1538491, 2018.

[13] S. Robra, R. SerpadaCruz, A. M. de Oliveira, J. A. A. Neto, and J. V. Santos, "Generation of biogas using crude glycerin from biodiesel production as a supplement to cattle slurry," *Biomass and Bioenergy*, vol. 34, no. 9, pp. 1330–1335, 2010.

[14] Y. Yang, S. Zheng, Z. Ai, and M. M. M. Jafari, "On the prediction of biogas production from vegetables, fruits, and food wastes by ANFIS- and LSSVM-based models," *BioMed Research International*, vol. 2021, Article ID 9202127, 8 pages, 2021.

[15] O. R. Dibaba, S. K. Lahiri, S. T'Jonck, and A. Dutta, "Experimental and artificial neural network modeling of a upflow anaerobic contactor (UAC) for biogas production from vinasse," *International Journal of Chemical Reactor Engineering*, vol. 14, no. 6, pp. 1241–1254, 2016.

[16] Y. Wang, T. Huntington, and C. D. Scown, "Tree-based automated machine learning to predict biogas production for anaerobic co-digestion of organic waste," *ACS Sustainable Chemistry & Engineering*, vol. 9, no. 38, Article ID 13000, 2021.

[17] M. O. Fajobi, O. A. Lasode, A. A. Adeleke, P. P. Ikubanni, and A. O. Balogun, "Investigation of physicochemical characteristics of selected lignocellulose biomass," *Scientific Reports*, vol. 12, no. 1, p. 2918, 2022.

[18] A. E. Ikpe, E. N. Akanu-Ibiam, and J. T. Promise, "Fuzzy modelling and optimization of anaerobic co-digestion Process parameters for effective biogas yield from bio-wastes," *The International Journal of Energy & Engineering Sciences*, vol. 5, no. 2, pp. 43–46, 2020.

[19] B. Heydari, E. Abdollahzadeh Sharghi, S. Rafiee, and S. S. Mohtasebi, "Use of artificial neural network and adaptive neuro-fuzzy inference system for prediction of biogas production from spearmint essential oil wastewater treatment in up-flow anaerobic sludge blanket reactor," *Fuel*, vol. 306, Article ID 121734, 2021.

[20] D. Erdirencelebi and S. Yalpir, "Adaptive network fuzzy inference system modeling for the input selection and prediction of anaerobic digestion effluent qualityfiuent Quality," *Applied Mathematical Modelling*, vol. 35, no. 8, pp. 3821–3832, 2011.

[21] S. O. Fabiano, F. Estevão, Q. Giovane, J. Maria, and O. C. Guimarães, "Comparative analysis of biogas production using artificial neural networks (ANNs) and classical methodologies," *American Journal of Engineering Research (AJER)*, vol. 8, no. 4, pp. 144–153, 2019.

[22] S. Kobra, M. K. Seyed, S. H. Fatemeh, and K. M. Farnoush, "Laboratory biogas production from kitchen wastes and applying an adaptive neuro-fuzzy inference system as a prediction model," *International Journal of Environment and Sustainable Development*, vol. 5, no. 3, 2014.

[23] S. Yalpir and G. Ozkan, "The development of a residential real-estate valuation model with ANFIS approach," *1st International Symposium on Computing in Science & Engineering*, vol. 17, pp. 10–20, Gediz University, Izmir, Turkey, 2010.

[24] M. Yilmaz, "Adaptive network based on fuzzy inference system estimates of geoid heights interpolation," *Scientific Resources, Essays*, vol. 5, pp. 2148–2154, 2010.

[25] A. P. Vassilopoulos and R. Bedi, "Adaptive neuro-fuzzy inference system in modelling fatigue life of multidirectional composite laminates," *Computational Materials Science*, vol. 43, no. 4, pp. 1086–1093, 2008.

[26] E. Buyukbingol, A. Sisman, M. Akyildiz, F. N. Alparslan, and A. Adejare, "Adaptive neuro-fuzzy inference system (ANFIS): a new approach to predictive modeling in QSAR applications: a study of neuro-fuzzy modeling of PCP-based NMDA receptor antagonists," *Bioorganic & Medicinal Chemistry*, vol. 15, no. 12, pp. 4265–4282, 2007.

[27] A. Mellit and S. A. Kalogirou, "ANFIS-based modelling for photovoltaic power supply system: a case study," *Renewable Energy*, vol. 36, no. 1, pp. 250–258, 2011.

[28] M. E. Keskin, D. Taylan, and O. Terzi, "Adaptive neural-based fuzzy inference system (ANFIS) approach for modelling hydrological time series," *Hydrological Sciences Journal*, vol. 51, no. 4, pp. 588–598, 2006.

[29] J. A. Olorunmaiye, I. K. Adegun, O. J. Ogunniyi, J. O. Aweda, T. K. Ajiboye, and S. Abdulkareem, "Effects of mixing ratios of cow dung, cassava peel and rice husk on thermodynamic properties of biogas," in *Anaerobic Digester Proceedings Of the iSTEAMS Multidisciplinary Cross-Border Conference*University of Professional Studies Accra Ghana, Madina, Ghana, 2016.

[30] S. S. Yaru, I. K. Adegun, and M. A. Akintunde, "Wobbe index determination of cattle dung biogas," *Scientia Agriculture*, vol. 9, no. 2, pp. 76–82, 2015.

[31] O. Ogunkunle, K. O. Olatunji, and A. Jo, "Comparative analysis of Co-digestion of cow dung and jatropha cake at ambient temperature," *Journal of Fundamentals of Renewable Energy and Applications*, vol. 08, no. 5, pp. 23–35, 2018a.

[32] M. M. Ghiasi, M. Arabloo, A. H. Mohammadi, and T. Barghi, "Application of ANFIS soft computing technique in modeling the CO_2 capture with MEA, DEA, and TEA aqueous solutions," *International Journal of Greenhouse Gas Control*, vol. 49, pp. 47–54, 2016.

[33] B. Najafi, S. Faizollahzadeh Ardabili, and S. F. Ardabili, "Application of ANFIS, ANN and logistic methods in estimating biogas production from spent mushroom compost (SMC)," *Resources, Conservation and Recycling*, vol. 133, pp. 169–178, 2018.

[34] S. Tiwari, R. Babbar, and G. Kaur, "Performance evaluation of two ANFIS models for predicting water quality index of river satluj (India)," *Advances in Civil Engineering*, vol. 2018, Article ID 8971079, 10 pages, 2018.

[35] M. A. Raharja, I. D. M. B. A. Darmawan, D. P. E. Nilakusumawati, and I. W. Supriana, "Analysis of membership function in implementation of adaptive neuro fuzzy inference system (ANFIS) method for inflation prediction," *Journal of Physics: Conference Series*, vol. 1722, no. 1, Article ID 12005, 2021.

[36] A. J. Adeyi, O. Adeyi, A. D. Ogunsola et al., "Moisture absorption characteristics and adaptive neuro-fuzzy modelling of ampelocissus cavicaulis fiber," *Reinforced Epoxy Composite LAUTECH Journal of Engineering and Technology*, vol. 14, no. 2, pp. 89–97, 2021.

[37] N. Talpur, M. N. M. Salleh, and K. Hussain, "An investigation of membership functions on performance of ANFIS for solving classification problems," *IOP Conference Series: Materials Science and Engineering*, vol. 226, Article ID 7012103, 2017.

[38] Present study, "Prediction of biogas yield from Co-digestion of lignocellulosic biomass using adaptive neuro-fuzzy inference system (ANFIS) model," 2022.

[39] Z. Zulkifi, S. Ismail, M. S. M. Zahari, N. A. Umor, and N. I. A. Aziz, "Screening on biogas optimization of lignocellulose-based materials using enzymatic hydrolysis process," *Chemical Engineering Transactions*, vol. 45, pp. 1585–1590, 2015.

[40] O. A. Makinde and L. O. Odokuma, "Comparative study of the biogas potential of plantain and yam peels," *British Journal of Applied Science & Technology*, vol. 9, no. 4, pp. 354–359, 2015.

[41] R. Amirta, E. Herawati, W. Suwinarti, and T. Watanabe, "Two-steps utilization of shorea wood waste biomass for the production of oyster mushroom and biogas – a zero waste approach," *Agriculture and Agricultural Science Procedia*, vol. 9, pp. 202–208, 2016.

[42] W. Prapinagsorn, S. Sittijunda, and A. Reungsang, "Co-digestion of napier grass and its silage with cow dung for methane production," *Energies*, vol. 10, p. 1654, 2017.

[43] D. Asante-Sackey, E. K. Tetteh, N. Nkosi et al., "Effects of inoculum to feedstock ratio in anaerobic digestion for biogas production," *International Journal of Hydrology*, vol. 2, no. 5, pp. 567–571, 2018.

[44] K. Madu and P. I. Onwuamaeze, "Evaluation of sawdust concentration on biogas production from sawdust waste, cow dung and water hyacinth," *Journal of Industrial Technology*, vol. 3, no. 1, pp. 41–46, 2018.

[45] R. Kargwal, Y. vika, M. K. Garg, K. Malik, and S. Mehta, "Effect of different concentration of paddy straw and cattle dung on biogas production," *International Journal of Current Microbiology and Applied Sciences*, vol. 8, no. 7, pp. 537–544, 2019.

[46] L. Wei, K. Qin, J. Ding et al., "Optimization of the co-digestion of sewage sludge, maize straw and cow manure: microbial responses and effect of fractional organic characteristics," *Scientific Reports*, vol. 9, no. 1, p. 2374, 2019.

[47] C. Vrabie, "Converting municipal waste to energy through the biomass chain, a key technology for environmental issues in (smart) cities," *Sustainability*, vol. 13, no. 9, p. 4633, 2021.

[48] S. Hirunsupachote, P. Kullavanijaya, and O. Chavalparit, "Biomethanation potential and enhancement of Acacia leaves waste via pretreatment and Co-digestion strategy," *Journal of Ecological Engineering*, vol. 23, no. 5, pp. 237–250, 2022.

[49] R. Ferrentino, M. Langone, D. Mattioli, L. Fiori, and G. Andreottola, "Investigating the enhancement in biogas production by hydrothermal carbonization of organic solid waste and digestate in an inter-stage treatment configuration," *Processes*, vol. 10, no. 4, p. 777, 2022.

[50] D. D. Keche, Z. M. Fetanu, W. Z. Babiso, and A. C. Wachemo, "Anaerobic digestion of urea pretreated water hyacinth removed from Lake Abaya; bio-methane potential, system stability, and substance conversion," *RSC Advances*, vol. 12, no. 14, pp. 8548–8558, 2022.

[51] S. O. Dahunsi, C. O. Osueke, T. M. A. Olayanju, and A. Lawal, "Co-digestion of theobroma cacao (cocoa) pod husk and poultry manure for energy generation: effects of pretreatment methods," *Bioresource Technology*, vol. 283, pp. 229–241, 2019.

[52] E. J. Eterigho, M. A. Musa, S. E. Ejejigbe, and T. S. Farrow, "Biogas production from rumen, municipal waste and Co-digested substrates: an opportunity for small and medium scale entrepreneurs (SME)," *IAENG Proceedings of the World Congress on Engineering 2021*, WCE 2021, London, U.K, 2021.

[53] O. O. Okediran, M. O. Fajobi, A. S. Onawumi et al., "Adaptive neuro-fuzzy modelling and prediction of academic performance of online distance learners in the era of covid-19," *International Journal of Multidisciplinary Research and Development*, vol. 8, no. 4, pp. 120–128, 2021.

[54] M. Kaveh, V. Rasooli Sharabiani, R. Amiri Chayjan, E. Taghinezhad, Y. Abbaspour-Gilandeh, and I. Golpour, "ANFIS and ANNs model for prediction of moisture diffusivity and specific energy consumption potato, garlic and cantaloupe drying under convective hot air dryer," *Information Processing in Agriculture*, vol. 5, no. 3, pp. 372–387, 2018.

[55] M. O. Fajobi, E. A. Awoyemi, D. T. Odedele, W. A. Adesope, and T. A. Adio, "Investigation of the relationship between stature and popliteal height sitting of Nigerian bus drivers," *Elixir International Journal; Elixir Mech. Engg.,* vol. 111, Article ID 48713, 2017.

[56] N. H. Che-Ithnin and H. Hashim, "Predictive modelling for biogas generation from palm oil mill effluent (pome)," *Chemical Engineering Transactions*, vol. 72, pp. 313–318, 2019.

[57] A. R. Fallahpour and A. R. Moghassem, "Yarn strength modelling using adaptive neuro-fuzzy inference system (ANFIS) and gene expression programming (GEP)," *Journal of Engineered Fibers and Fabrics*, vol. 8, no. 4, Article ID 155892501300813, 2013.

[58] S. Jaroenpoj, Q. J. Yu, and J. Ness, "Development of artificial neural network models for biogas production from co-digestion of leachate and pineapple peel," *The Global Environmental Engineers*, vol. 1, pp. 42–47, 2014.

[59] S. Uzuner and D. Cekmecelioglu, "Comparison of artificial neural networks (ANN) and adaptive neuro-fuzzy inference system (ANFIS) models in simulating polygalacturonase," *Bioresources*, vol. 11, no. 4, pp. 8676–8685, 2016.

[60] Y. Tao, Y. Li, R. Zhou et al., "Neuro-fuzzy modeling to predict physicochemical and microbiological parameters of partially dried cherry tomato during storage: effects on water activity, temperature and storage time," *Journal of Food Science Technology Springer*, vol. 53, no. 10, pp. 3685–3694, 2016.

[61] A. F. Mashaly and A. A. Alazba, "Membership function comparative investigation on productivity forecasting of solar still using adaptive neuro-fuzzy inference system approach," *Environmental Progress & Sustainable Energy*, vol. 37, no. 1, pp. 249–259, 2018.

[62] M. Babanezhad, A. T. Nakhjiri, A. Marjani, M. Rezakazemi, and S. Shirazian, "Evaluation of product of two sigmoidal membership functions (psigmf) as an ANFIS membership function for prediction of nanofluid temperature," *Scientific Reports*, vol. 10, no. 1, Article ID 22337, 2020.

[63] S. O. Sada and S. C. Ikpeseni, "Evaluation of ANN and ANFIS modelling ability in the prediction of AISI 1050 steel machining performance," *Heliyon*, vol. 7, no. 2, Article ID 06136, 2021.

[64] A. Makolo and R. Olapojoye, "Bayesian-ANFIS student model for an intelligent tutoring system," *International Journal of Applied Information Systems*, vol. 12, no. 37, pp. 16–22, 2021.